Published in final edited form as:

Ann Neurol. 2015 November ; 78(5): 787–800. doi:10.1002/ana.24517.

Validating novel tau PET tracer [F-18]-AV-1451 (T807) on postmortem brain tissue

Marta Marquie, MD[1,2,3], **Marc D. Normandin, PhD**[4], **Charles R. Vanderburg, PhD**[1,2,5], **Isabel Costantino, BA**[1,2], **Elizabeth A. Bien, BS**[1,2,5], **Lisa G. Rycyna, BS**[1,2,5], **William E. Klunk, MD, PhD**[6], **Chester A. Mathis, PhD**[7], **Milos D. Ikonomovic, MD**[8,9], **Manik L. Debnath, MS**[6], **Neil Vasdev, PhD**[4], **Bradford C. Dickerson, MD**[2], **Stephen N. Gomperts, MD, PhD**[1,2], **John H. Growdon, MD**[2], **Keith A. Johnson, MD**[2], **Matthew P. Frosch, MD, PhD**[1,2,10], **Bradley T. Hyman, MD, PhD**[1,2,5], and **Teresa Gomez-Isla, MD, PhD**[1,2]

[1]MassGeneral Institute for Neurodegenerative Disease, Charlestown, MA

[2]Department of Neurology, Massachusetts General Hospital, Boston, MA

[3]Autonomous University of Barcelona, Medicine Doctoral Studies, Barcelona, Spain

[4]Center for Advanced Medical Imaging Sciences, Division of Nuclear Medicine and Molecular Imaging, Department of Radiology, Massachusetts General Hospital, Harvard Medical School, Boston, MA

[5]Harvard NeuroDiscovery Center, Harvard Medical School, Boston, MA

[6]Department of Psychiatry, University of Pittsburgh School of Medicine, Pittsburgh, PA

[7]Department of Pharmacology and Chemical Biology, University of Pittsburgh School of Medicine, Pittsburgh, PA

[8]Department of Neurology, University of Pittsburgh School of Medicine, Pittsburgh, PA

[9]Geriatric Research Education and Clinical Center, VA Pittsburgh Clinical System, Pittsburgh, PA

[10]C.S. Kubik Laboratory for Neuropathology, Massachusetts General Hospital, Boston, MA

Abstract

Corresponding author: Teresa Gomez-Isla, MD, PhD. Department of Neurology, Massachusetts General Hospital. WACC, Suite 715, 15th Parkman St., Boston MA 02114, USA. Tel. +1.617.643-5562. Fax. +1.617.726-4101. tgomezisla@mgh.harvard.edu.

Author's contributions to the study:

MM, MN, CV, MF, BH, TGI: conception and design of the study; data collection and analysis; writing the manuscript. IC, EB, LR, CM, MD, NV, BD, SN, JG: data collection and analysis. WK, MI: data collection and analysis; writing the manuscript. KJ: conception and design of the study; data collection and analysis.

Potential conflict of interest:

MM, MN, CV, IC, EB, LR, WK, CM, MI, MD, BD, SG, JG, MP, TGI have no conflicts of interest.

NV has a patent called "Improved Radiosynthesis of The Tau Imaging Radiopharmaceutical [18F]AV-1451" (PCT/US2014/040165) pending. AV-1451 is the PET compound used in this study.

KJ reports grants from Eli Lilly and Company during the conduct of the study. Eli Lilly and Company owns Avid, the company that created AV-1451, the PET compound used in this study.

BH reports personal fees from Eli Lilly and Company outside the submitted work. Eli Lilly and Company owns Avid, the company that created AV-1451, the PET compound used in this study.

Objective—To examine region and substrate-specific autoradiographic and *in vitro* binding patterns of PET tracer [F-18]-AV-1451 (previously known as T807), tailored to allow *in vivo* detection of paired helical filament tau-containing lesions, and to determine whether there is off-target binding to other amyloid/non-amyloid proteins.

Methods—We applied [F-18]-AV-1451 phosphor screen autoradiography, [F-18]-AV-1451 nuclear emulsion autoradiography and [H-3]-AV-1451 *in vitro* binding assays to the study of postmortem samples from patients with a definite pathological diagnosis of Alzheimer's disease, frontotemporal lobar degeneration-tau, frontotemporal lobar degeneration-TDP-43, progressive supranuclear palsy, corticobasal degeneration, dementia with Lewy bodies, multiple system atrophy, cerebral amyloid angiopathy and elderly controls free of pathology.

Results—Our data suggest that AV-1451 strongly binds to tau lesions primarily made of paired helical filaments in Alzheimer's brains e.g. intra and extraneuronal tangles and dystrophic neurites, but does not seem to bind to a significant extent to neuronal and glial inclusions mainly composed of straight tau filaments in non-Alzheimer tauopathy brains or to β-amyloid, α-synuclein or TDP-43-containing lesions. AV-1451 off-target binding to neuromelanin- and melanin-containing cells and, to a lesser extent, to brain hemorrhagic lesions was identified.

Interpretation—Our data suggest that AV-1451 holds promise as surrogate marker for the detection of brain tau pathology in the form of tangles and paired helical filament-tau-containing neurites in Alzheimer's brains but also point to its relatively lower affinity for lesions primarily made of straight tau filaments in non-Alzheimer tauopathy cases and to the existence of some AV-1451 off-target binding. These findings provide important insights for interpreting *in vivo* patterns of [F-18]-AV-1451 retention.

Introduction

The first novel paired helical filament (PHF)-tau targeting positron emission tomography (PET) tracers, such as [F-18]-AV-1451 (previously known as T807), have been demonstrated to detect tangle pathology *in vivo*,[1] opening an exciting opportunity of using them as a potential surrogate marker to measure tau-bearing neurofibrillary lesions in the brain by *in vivo* neuroimaging. An anticipated barrier to progress in the field of *in vivo* tau imaging is the need for tracers with high binding selectivity for tau lesions relative to β-amyloid (Aβ) plaques and other amyloid-like proteins with a β-pleated sheet conformation. A recent study suggested that PET tracer [F-18]-AV-1451 is highly selective for tau over Aβ with negligible off-target binding.[2] Xia and colleagues suggested that the autoradiography pattern of [F-18]-AV-1451 correlates better with PHF-tau immunoreactivity than with Aβ immunostaining.[1] Emerging data from *in vivo* human [F-18]-AV-1451 PET scans showed significantly higher AV-1451 retention across frontal, parietal and temporal cortices and the hippocampus in Alzheimer's (AD) patients when compared to individuals with mild cognitive impairment (MCI) and cognitively normal control subjects.[3] A comprehensive postmortem validation of this novel PET tracer is critical for determining its usefulness for antemortem diagnosis and staging of AD and other tauopathies, and to understand exactly what the retention of [F-18]-AV-1451 in PET studies means in terms of neuropathological substrate.

The presence of brain aggregates of abnormally hyperphosphorylated tau in the form of filaments and neurofibrillary tangles (NFT) is a defining pathological hallmark of AD and other tauopathies, such as some types of frontotemporal lobe degeneration (FTLD)-tau including Pick's disease (PiD),[4] progressive supranuclear palsy (PSP)[5] and corticobasal degeneration (CBD).[6] While these various disorders differ in terms of the regional distribution of tau deposits in the brain, there are other important differences as well which are potentially associated with altered ability to be identified by [F-18]-AV-1451. In these disorders, tau aggregates differ in their morphology: NFT, neuropil threads and dystrophic neurites associated with neuritic plaques in AD; Pick bodies in PiD; globose tangles, coiled bodies and tufted astrocytes in PSP; and astrocytic plaques, coiled bodies and neuropil threads in CBD. In addition, these diseases differ according the tau isoform composition of the aggregates: a mixture of three (3R) and four repeat (4R) tau isoforms in AD; 3R in PiD; and 4R in both PSP and CBD. Finally, the ultrastructural characteristics of tau filaments differ across diseases: PHF in AD versus mainly straight filaments in PiD, PSP and CBD.[7–9]

Because AV-1451 was initially screened to specifically detect tau in the form of PHF,[1] we predicted that this tracer would exhibit high binding affinity and selectivity for PHF-tau lesions relative to non-PHF-tau lesions, Aβ deposits and α-synuclein and transactive response DNA binding protein-43 (TDP-43) aggregates. To validate the site/s of AV-1451 binding and determine whether there is off-target binding, we carefully examined the regional and substrate-specific autoradiograhic patterns of [F-18]-AV-1451 by using legacy postmortem brain, retina and skin tissue samples. Cases with a definite pathological diagnosis of AD, FTLD-tau (PiD, PSP, CBD), FTLD-TDP-43, CAA, synucleinopathies (dementia with Lewy bodies (DLB) and multiple system atrophy (MSA)), metastatic melanoma, brain hemorrhages, superficial siderosis and controls free of pathology were included in this study. *In vitro* binding levels of [H-3]-AV-1451 using homogenates prepared from the same brain tissue material were also analyzed. Our results suggest that AV-1451 holds promise as a surrogate marker for the detection of brain PHF tau-bearing neurofibrillary lesions by *in vivo* imaging in the setting of some off target non-neurodegenerative lesion binding as well.

Methods

Tissue samples

Postmortem brain tissue from 24 subjects from the Massachusetts Alzheimer's Disease Research Center (MADRC) Neuropathology Core was included in this study. Additional retina and skin tissue samples were also analyzed. Autopsies were performed according to standardized protocols[10] and tissue collection and use was approved by the local Institutional Review Board. The pathological diagnosis in the cohort were as follows: AD[11] (n=3), normal control (n=2), diffuse cerebral amyloid angiopathy (CAA) carrier of the D23N Iowa APP mutation[12] (n=1), PiD[4] (n=3), PSP[5] (n=3), CBD[6] (n=2), DLB[13] (n=3), multiple systemic atrophy[14] (MSA, n=2), FTLD-TDP-43[4] (n=1), brain metastatic melanoma[15] (n=1), superficial siderosis[16] (n=1), and brain hemorrhages (n=2). Histological evaluation of each case was routinely performed on a specific set of 19 blocked regions representative for a spectrum of neurodegenerative diseases. All paraffin-embedded blocks were stained with

luxol fast blue and hematoxylin and eosin (H&E), while selected blocks were routinely stained for Bielschowsky silver stain and Aβ, α-synuclein, ubiquitin, TDP-43 and phospho-tau immunoreactivity. In addition to human samples, brains from adult (12 month old) rTg4510 mice (n=2) and age-matched wild type non-transgenic littermates (WT, n=2) were included in the study. rTg4510 is a well-characterized tauopathy mouse model that overexpresses a human mutant form of tau (P301L) linked to familial FTDL.[17, 18] rTg4510 mice develop cortical NFT, mainly composed of straight tau filaments, by the age of 4 months.[17]

Blocks of frozen brain tissue containing frontal, parietal, temporal and occipital cortices, hippocampal formation, entorhinal cortex (EC), cingulate, cerebellum, basal ganglia and midbrain were cut into sections 10μm-thick in a cryostat (Thermo-Shandon SME Cryostat), mounted on Histobond adhesion slides (StatLab, TX) and used for [F-18]-AV-1451 phosphor screen and high resolution nuclear emulsion autoradiography and for fluorescence staining. Adjacent blocks of frozen tissue were homogenized and used for *in vitro* [3-H]-AV-1451 binding assays.

[F-18]-AV-1451 phosphor screen autoradiography

[F-18]-AV-1451 was synthesized as previously described by us.[19] [F-18]-AV-1451 phosphor screen autoradiography was performed following a slightly modified version of a previously published protocol.[1] In brief, 10μm-thick frozen brain sections were fixed in 100% methanol at room temperature for 20 minutes and then transferred to a bath containing high specific activity [F-18]-AV-1451 in 10mM PBS with a radioactivity concentration of approximately 20 μCi/ml. Adjacent brain slices were placed in a bath that was identical in all aspects except that unlabeled AV-1451 was added to yield 1 μM chemical concentration, a blocking condition sufficient to saturate essentially all available specific binding sites of tau.[1] After incubation for 60 minutes, racks of slides were removed from the respective radioactive solutions and briefly incubated in a series of wash baths to remove unbound radiotracer. Wash solutions and incubation times were: 10 mM PBS for 1 minute, 70% ethanol/30% PBS for 2 minutes, 30% ethanol/70% PBS for 1 minute, and lastly 100% 10 mM PBS for 1 minute. Racks were removed from the final wash solution and slices were allowed to air dry before transfer of the slides to a storage phosphor screen (Multi Sensitive Phosphor Screen, PerkinElmer Life and Analytic Sciences, Shelton, CT) that had been photobleached immediately prior by exposure on a white light box for a minimum of 15 minutes. The slides and phosphor screen were enclosed in an aluminum film cassette and set in a dark area away from sources of radioactivity for the duration of the overnight exposure period. Under dim lighting conditions, the cassette was opened and the slides removed from the exposed screen, which was mounted to the carousel of the digital imaging system (Cyclone Plus Storage Phophor Scanner, PerkinElmer Life and Analytic Sciences). Scanning of screens was controlled by the manufacturer's OptiQuant software package using the highest available resolution of 600 dpi (approximately 42 micron sampling interval). Digital images were saved in uncompressed form at full resolution and pixel depth. Images from adjacent brain slices incubated in the unblocked (high specific activity [F-18]-AV-1451 only) and blocking ([F-18]-AV-1451 plus 1 μM unlabeled AV-1451) conditions were compared to determine total and non-specific binding of [F-18]-AV-1451 in the tissue.

[F-18]-AV-1451 nuclear emulsion autoradiography

Coating of the slides with a liquid photographic emulsion was performed in adjacent frozen cryostat sections to those used for phosphor screen autoradiography in order to obtain autoradiographic information at the cellular resolution level.[20–22] In brief, the slides were fixed in 100% methanol, incubated with [F-18]-AV-1451 for 60 minutes, washed with PBS and ethanol and air dried (as described above). The slides were then dipped in the nuclear photographic emulsion (1:5 dilution in H_2O, Ilford nuclear research emulsion K.5, Polysciences, Warrington, PA) in a dark room and left overnight laying flat in a dark box. The next day the slides were developed for 4 minutes (Ilford Phenisol developer), placed in a bath with 1% acetic acid to stop the reaction for 2 minutes, transferred to a fixative solution for 4 minutes (Ilford Hypam fixer), and finally washed in distilled H_2O twice for 5 minutes. Immunohistochemistry was then performed on the nuclear emulsion-dipped sections. First the sections were washed for 5 minutes with PBS, then incubated with 2.5% normal horse blocking serum for 20 minutes, followed by the appropriate primary antibody - anti-tau PHF-1 (1:100, mouse, kind gift of Dr. Peter Davies), anti-Aβ (1:50, rabbit, IBL), anti α-synuclein (1:100, mouse, Zymed) or anti-TDP-43 (1:100, rabbit, Protein Tech) - for 40 minutes at 37°C. The sections were then washed with PBS twice for 2 minutes, and then incubated with the secondary antibody (ImmPRESS™ anti-mouse IgG (Vector Laboratories product MP-2400, Burlingame, CA or ImmPRESS™ anti-rabbit Ig (Vector Laboratories product MP-7401, Burlingame, CA)) for 40 minutes at 37°C. The sections were washed again with PBS twice for 2 minutes, and then developed with DAB solution (Vector Laboratories product SK-4100) for 4 minutes. H&E was used for counterstaining. The slides were washed again with PBS twice for 2 minutes, then dehydrated and cleared through a graded ethanol series into xylene and cover-slipped with Permount mounting medium (Fisher Scientific, US). Photomicroscopy was performed on an upright Olympus BX51 (Olympus, Denmark) microscope using visible light.

[H-3]-AV-1451 binding assay

Fresh-frozen human brain samples were homogenized with a Polytron tissue homogenizer (PT 10/35; Brinkman Instruments, Westbury, NY) at room temperature for 30 seconds at setting 6 in PBS (137 mM NaCl, 3 mM KCl, 10mM sodium phosphate, pH 7.0) at a concentration of 10 mg of brain per milliliter. The homogenates were aliquoted and frozen at 80°C until used for binding assays within 2 months. No significant changes in binding characteristics have been observed in samples assayed repeatedly over this time period. 10 mg/ml frozen brain homogenate aliquots were thawed and diluted 10-fold in binding buffer to 1 mg/ml. 500 μl of appropriate concentrations of non-radioactive compound to be tested were combined with 400 μl of [H-3]-AV-1451 (29.7 Ci/mmol; gift of Avid Radiopharmaceuticals, Inc., a wholly owned subsidiary of Eli Lilly and Company) in a volume of 900 μl of binding buffer. The assay began by addition of 100 μl of the 1 mg/ml brain homogenate to achieve a final concentration of 0.10 mg tissue/ml for all radioligands. The final concentration of [H-3]-AV-1451 is typically 1–2 nM. After incubation at room temperature for 60 minutes, the binding mixture was filtered through a Whatman GF/B glass filter via a Brandel M-24R cell harvester and rapidly washed 5 times with 3 ml binding buffer. The filters were counted in Cytoscint-ES after sitting in the cocktail overnight.

Complete (100%) inhibition of binding was defined as the number of counts displaced by 3 μM non-radioactive AV-1451. All assays were done in triplicate.

Results

A summary of the demographic characteristics of the postmortem brain samples studied is shown in Table 1.

[F-18]-AV-1451 phosphor screen autoradiography

Phosphor screen autoradiography experiments using [F-18]-AV-1451 (aliquots from material prepared from *in vivo* imaging on the same day) revealed strong binding in the hippocampal formation and EC, frontal, temporal, parietal and occipital cortices from brain slices containing NFT in AD cases (Figure 1A). Of note, binding was almost completely blocked after incubating the slides with 1μM unlabeled AV-1451, demonstrating the specificity of the signal. No signal was detected in the white matter or other non-tangle containing regions in AD cases, with the exception of the substantia nigra (Figure 2E), as discussed further below. Slides from control brains free of neurofibrillary pathology showed no AV-1451 signal in any of the cases analyzed (Figure 1B), except for the substantia nigra (Figure 2E) as in AD and the rest of the cases analyzed. No AV-1451 binding was detected in the cerebellum (Figure 1A), a region that is typically used in neuroimaging studies as a reference region devoid of specific binding, or in the basal ganglia (Figure 1B), in any of the cases studied. We also noticed the absence of detectable AV-1451 binding in brain slices containing non-PHF tau lesions from PiD (Figure 1C), PSP (Figure 1D) and CBD (Figure 1E) cases when compared to control brains. Of note, incidental AV-1451 binding to age-related PHF-tangles in the entorhinal cortex was noted in these non-AD cases with NFT Braak stage II, and served as an internal positive control as it is shown in the PSP case illustrated in Figure 1D. Similarly, we could not detect labeling in the brains of aged rTg4510 mice that contain innumerable P301L (4R) tau neurofibrillary lesions (Figure 1F). The absence of detectable labeling of tau lesions in the mouse model and in the non-AD tauopathies, which share the feature of primarily straight filaments of tau rather than PHF, suggests that AV-1451 has a higher affinity and specificity for PHF-tau. Importantly, brain slices from the D23N Iowa APP mutation carrier[12] displaying very severe CAA pathology completely lacked [F-18]-AV-1451 autoradiographic signal (Figure 2A) and were indistinguishable from control brain slices. This favors the idea that AV-1451 binds with much stronger affinity and selectivity to PHF-tau containing slices than Aβ lesion-containing ones, as it had been suggested in the previous study by Xia and colleagues.[1] Brain slices containing TDP-43 inclusions in FTLD-TDP-43 cases (Figure 2B) and α-synuclein lesions in DLB (Figure 2C) and MSA (Figure 2D) cases, respectively, also lacked detectable AV-1451 binding on phosphor screen autoradiography in all regions studied, with the exception of the substantia nigra (Figure 2E), as noted in all other cases analyzed including controls, and of the incidental age-related PHF-tangle pathology confined to the entorhinal cortex and limbic regions in cases with NFT Braak stages II–III. Of note, this universal and strong binding of [F-18]-AV-1451 to midbrain slices containing substantia nigra, regardless of the presence of underlying tau aggregates, was blocked almost completely when incubating the slides with 1μM unlabeled AV-1451 (Figure 2E), strongly pointing to the substantia nigra as a brain region where

AV-1451 has a robust off-target binding. In addition to the substantia nigra, and to a lesser extent, some [F-18]-AV-1451 binding was also noticed in brain slices containing parenchymal and subarachnoidal hemorrhages (Figure 4F–G), suggesting the possibility of some AV-1451 binding also to this type of lesion. No labeling could be detected however in a case with superficial siderosis with iron deposition in the setting of chronic vascular leakage of red blood cells (Figure 4E).

[F-18]-AV-1451 nuclear emulsion autoradiography

In order to further confirm the above observations and to obtain cellular resolution, we dipped adjacent brain slices to those used in phosphor screen autoradiography in a photographic nuclear emulsion. When slices are developed, silver grains struck by positrons emitted during [F-18] nuclear decay are visualized allowing the identification of [F-18]-AV-1451 labeled lesions below the silver grains of the emulsion by optical microscopy.

Using this method, we confirmed that tissue sections from AD cases containing hippocampal formation, EC, and frontal, parietal, temporal and occipital cortices displayed a strong and selective concentration of silver grains, reflecting underlying [F-18]-AV-1451 binding in the grey matter with a negligible presence of silver grains in the white matter (Figure 3A left panel). The distribution of silver grains in those areas closely mirrored the pattern of PHF-1 immunostaining reactivity on adjacent slices with the highest amount of silver grains being observed in cortical layers III and V, as one would expect based on the well known robust density of tangle lesions in those cortical layers in AD[23, 24] (Figure 3A middle panel), rather than the more scattered plaque distribution pattern revealed by Aβ immunostaining (Figure 3A right panel). [F-18]-AV-1451 nuclear emulsion autoradiography followed by immunostaining with PHF-1 or Aβ antibodies on the same brain slices was also performed. This further confirmed that [F-18]-AV-1451 labeled lesions below the silver grains of the emulsion were PHF-tau containing lesions, including classic NFT (Figure 3B left panel), both intra and extraneuronal e.g. “ghost tangles” (Figure 3B middle panel), and PHF-tau containing neurites (Figure 3B right panel), but not Aβ plaques (Figure 3C) or amyloid-laden vessels (Figure 3D).

In agreement with the results obtained by phosphor screen autoradiography, brain slices from control brains free of neurofibrillary pathology did not show detectable accumulations of silver grains in any of the cortical brain regions examined (data not shown). Similarly, a negligible number of silver grains were observed colocalizing with tau containing lesions in rTg4510 mouse brains (Figure 3E) and in PiD (Figure 3F), PSP (Figure 3G) and CBD (Figure 3H) cases, further strengthening the relatively higher affinity and selectivity of AV-1451 for tau lesions primarily composed of PHF (as seen in AD) compared to those mainly made of straight filaments of tau in non-AD tauopathies and rTg4510 mice. In addition, no silver grains were observed colocalizing with α-synuclein (Figure 3I–J) or TDP-43 containing inclusions (Figure 3K).

Importantly, neuromelanin-containing neurons in the substantia nigra pars compact a (Figure 4A), melanin-containing retinal pigment epithelium (RPE) cells (Figure 4C), as well as leptomeningeal melanocytes (not shown), skin melanocytes (Figure 4B) and malignant melanocytes in a metastatic melanoma (Figure 4D) consistently demonstrated robust

concentration of silver grains independent of any tau aggregates. This identified a prominent off-target binding activity of AV-1451 to both neuromelanin and melanin-containing cells. To a lesser extent, a slight AV-1451 signal was also seen in association with acute and subacute parenchymal (Figure 4F) and subarachnoid (Figure 4G) hemorrhages, pointing to some additional [F-18]-AV-1451 off-target binding in these lesions. Interestingly, no [F-18]-AV-1451 signal was detected in the superficial siderosis case containing multiple hemosiderin deposits (Figure 4E) suggesting that the age of the hemorrhages (e.g. acute/subacute vs chronic) could be a factor in the observed variable range of tracer's binding to these lesions.

[H-3]-AV-1451 binding assays

The binding levels derived from [H-3]-AV-1451 *in vitro* binding assays conducted in frozen brain homogenate aliquots representing multiple brain regions across cases are shown in Table 2. Overall, and in agreement with the results obtained from the autoradiography experiments described above, our [H-3]-AV-1451 *in vitro* binding assay revealed higher levels of tracer binding in the majority of PHF-tangle containing regions analyzed in AD brains when compared to non-AD tauopathy cases, CAA, α-synuclein, TDP-43 lesion-containing brain tissue samples and control brains. However, the numerical differences in the ligand binding levels between AD and non-AD brains detected by this method seemed relatively narrow and the signal-to-noise ratio relatively low when compared to the robust differential patterns of binding observed when applying autoradiographic techniques. This may be due to the fact that the high ethanol concentrations (30–70%) used in the autoradiographic studies is much more effective at washing out non-specific binding than the PBS washes used in the homogenate binding studies. Of note, the highest binding values in the [H-3]-AV-1451 *in vitro* binding assay were detected in the metastatic melanoma and the cases with brain parenchymal and subarachnoid hemorrhages, further pointing to these lesions as AV-1451 off-target binding substrates.

Discussion

To understand exactly what [F-18]-AV-1451 PET positivity means in terms of neuropathological substrate, we have carefully characterized the autoradiographic and *in vitro* binding patterns of this novel tracer in postmortem tissue samples representing a broad spectrum of neurodegenerative pathologies. Our observations, derived from combined [F-18]-AV-1451 sensitive autoradiography and immunohistochemistry and from [H-3]-AV-1451 *in vitro* binding assays, suggest that AV-1451 strongly binds to lesions primarily made of tau in the form of PHF in tissue samples from brains with AD (intra- and extraneuronal tangles and PHF-tau containing neurites), but does not bind to a significant extent to neuronal and glial inclusions mainly composed of straight tau filaments in tissue samples from brains with non-AD tauopathy lesions or to Aβ, α-synuclein or TDP-43-containing lesions. Importantly, a pronounced off-target binding of AV-1451 to neuromelanin- and melanin-containing cells and, to a lesser extent, to acute and subacute brain hemorrhagic lesions, was identified in this study suggesting that these substrates represent non-specific binding sites of this tracer, and this should be taken carefully into account when interpreting the AV-1451 retention patterns observed by *in vivo* neuroimaging.

The PET tracer AV-1451 originally came out of compound library screens that used human brain slices laden with PHF-tau tangles as the binding target.[1] Early studies suggested that this compound had more than 29-fold higher affinity for PHF-tau over Aβ, with non-detectable binding to off-target proteins.[2] The first emerging data from *in vivo* human [F-18]-AV-1451 PET scans pointed to a significantly higher AV-1451 retention the brain of patients with AD when compared to individuals with MCI and cognitively normal control subjects.[3] In agreement with these observations, our recent *in vivo* studies based on [F-18]-AV-1451 PET and amyloid-β PET using Pittsburgh Compound B (PiB) in older clinically normal individuals and symptomatic patients with MCI or mild AD dementia have also shown high cortical [F-18]-AV-1451 retention in patients with MCI and AD dementia compared to clinically normal controls, suggesting that AV-1451 could have value as a biomarker that reflects tau pathology in AD brains (Johnson K, Becker A, Sepulcre J et al. Initial experience with F18 T807-Tau PET imaging along the spectrum of normal aging and Alzheimer's disease dementia. Presented in: Human Amyloid Imaging. Miami, Florida, 2014).

This compound is now quickly making its way into use in clinical research including secondary prevention trials in AD like the A4 trial.[25] Thus, a careful study to validate the sensitivity and specificity of this novel tracer, and to exactly define the underlying pathological burden responsible for *in vivo* [F-18]-AV-1451 PET retention is particularly important at this time. Based on the observations above, we predicted that AV-1451 would bind with high affinity and specificity to tau assemblies in the form of tangles of PHF and would show little or no binding affinity to straight filaments lesions or to other abnormal protein aggregates primarily made of Aβ, α-synuclein or TDP-43. To unequivocally confirm or disprove this hypothesis we used three different methods ([F-18]-AV-1451 phosphor screen autoradiography, [F-18]-AV-1451 nuclear emulsion autoradiography and [H-3]-AV-1451 *in vitro* binding assays) applied to the study of a series of autopsy samples from individuals with a definitive diagnosis of AD, CAA, PiD, PSP, CBD, FTLD-TDP-43, DLB, MSA and control brains free of neurodegenerative pathology.

Our results from phosphor screen autoradiography and nuclear photographic emulsion, both using [F-18]-AV-1451, confirmed that while AV-1451 avidly bound to PHF-tangle containing slices from AD brains, it failed to label CAA, α-synuclein and TDP-43 lesion-containing slices as well as slices from control brains free of pathology. Importantly, [F-18]-AV-1451 also failed to label tau-containing lesions in slices from non-AD tauopathy brains and from rTg4510 mice. Thus, our data suggest that this tracer has greater selectivity for PHF-tau over tau aggregates that are primarily made of straight filaments in non-AD tauopathies. The unequivocally positive labeling in these autoradiographic experiments of incidental age-related PHF-tangles in the entorhinal cortex (NFT Braak stage II) of human non-AD brains, served as an optimal internal positive control. The regional and laminar autoradiographic patterns of distribution of [F-18]-AV-1451, as revealed by the combination of autoradiography using a fine grain nuclear emulsion and immunohistochemistry, closely matched those of classic PHF-tangles in AD brains[23, 24] demonstrating very low nonspecific binding to the whiter matter and a strong labeling in particular of cortical layers III and V. We confirmed that [F-18]-AV-1451-labeled lesions below the silver grains of the emulsion were PHF-tau containing lesions, including neurofibrillary tangles, both intra and

extraneuronal e.g. “ghost tangles” and PHF-tau containing neurites decorating the periphery of dense cored plaques, further pointing to these lesions as the main pathological substrate of [F-18]-AV-1451 signal detected by *in vivo* neuroimaging. The microscopic examination of diffuse plaques, CAA, non-PHF tau lesions, α-synuclein and TDP-43 aggregates confirmed the absence of detectable accumulation of silver grains of the photographic emulsion associated with those lesions, favoring the relative specificity of AV-1451 for PHF-tau aggregates over β-amyloid plaques and other abnormal protein brain deposits with a β-pleated sheet conformation. In agreement with these autoradiographic findings, our [H-3]-AV-1451 *in vitro* binding assay showed higher levels of binding in PHF-tangle containing regions in AD brains when compared to non-AD tauopathy brains, CAA, α-synuclein, TDP-43 lesion-containing brains and controls, although the magnitude of the difference detected by this method seemed substantially less robust than that observed by autoradiography. As discussed further below, we believe that nonspecific binding of AV-1451 to sample components such as hemoglobin and the absence of an ethanol washing step in this assay could contribute, at least in part, to explain the background noise and the relatively modest signal-to-noise ratio of the [H-3]-AV-1451 *in vitro* binding assay used here.

Intriguingly, our recent *in vivo* studies showed particularly high levels of AV-1451 retention in the inferior temporal cortex and parieto-occipital association cortical areas in MCI and AD patients, and relatively lower AV-1451 retention in medial temporal lobe structures like the hippocampal formation or the entorhinal cortex (Johnson K, Becker A, Sepulcre J et al. Initial experience with F18 T807-Tau PET imaging along the spectrum of normal aging and Alzheimer’s disease dementia. Presented in: Human Amyloid Imaging. Miami, Florida, 2014). It has long been known, from pathological studies of AD brains, that while PHF-tangle densities in AD are highest in the medial temporal lobe, the load of neuritic plaques, and thus of PHF-tau containing neurites, is in fact relatively low in those brain regions with the highest density of these lesions as well as neuropil threads being consistently found in temporal, parietal and occipital association cortices in AD.[24] Thus, our finding that AV-1451 binds to PHF-tau containing neurites in addition to classic PHF-tangles, may provide an explanation for the regional pattern of retention noticed *in vivo* in MCI and AD patients.

Another intriguing but frequent finding emerging from early [F-18]-AV-1451 PET imaging studies is the abnormally high binding of this tracer observed in the midbrain, the basal ganglia and the eyes, in a significant proportion of individuals with diverse clinical diagnoses and across the entire spectrum of cognition from demented to cognitively normal (Keith Johnson personal communication). The results of our nuclear emulsion autoradiography studies provide an explanation for these *in vivo* findings and demonstrate that AV-1451 not only binds to PHF-tau aggregates but also exhibits some off-target binding, in particular to neuromelanin-containing cells including pigmented neurons in the substantia nigra (regardless of the presence or absence of nigral tau pathology). Even though it is well known that neuromelanin and melanin are distinct, during the course of our experiments, we noticed, along with off-target binding to neuromelanin containing cells, an incidental strong binding of AV-1451 to extracutaneous melanocytes located in the leptomeninges. This observation prompted us to examine melanin-containing retinal pigment epithelium cells, skin melanocytes and lesions containing malignant melanocytes where we also observed

prominent off-target binding. Our data also suggest that AV-1451 exhibits some weaker off-target binding to parenchymal and subarachnoid hemorrhages, and this could be particularly relevant for the correct interpretation of AV-1451 *in vivo* neuroimaging in patients with brain hemorrhagic lesions. Intriguingly, even though high *in vivo* retention of AV-1451 in the basal ganglia has been noticed in approximately 30–50% of individuals across ages and clinical diagnoses (Keith Johnson personal communication), no detectable [F-18]-AV-1451 binding to basal ganglia was observed by autoradiography in any of the cases studied here, regardless of the presence of robust amounts of tau aggregates in some of the non-AD tauopathy cases. This suggests that either the *in vivo* tracer uptake in this brain region may represent non-specific binding influenced by biological or technical factors other than underlying tau pathology or that the ethanol washing steps used in the autoradiographic studies removed [F-18]-AV-1451 labeling from the basal ganglia samples.

We also conducted exploratory studies with two AV-1451 fluorescent analogues, T726 and T557 (kindly provided by Avid Radiopharmaceuticals, Inc.), that share a similar but not identical structure to the parent compound AV-1451 which is not fluorescent itself.[2] Of note, histological staining with these fluorescent compounds required concentrations 3–5 orders of magnitude higher than AV-1451 in autoradiography due to their low signal intensity. Not unexpectedly, these fluorescent analogues not only labeled tangles and PHF-containing neurites, but also non-PHF tau lesions, amyloid plaque cores and amyloid-laden vessels (data not shown). The labeling of non-PHF tau and amyloid-containing lesions by AV-1451 fluorescent analogues is most likely due to a concentration-dependent specificity that is lost at the very high concentrations necessary for fluorescence studies. The results obtained from autoradiography experiments using the actual parent compound [F-18]-AV-1451 at similar concentrations used *in vivo* for PET studies, as described above, support this notion. Even though we cannot completely rule out the possibility of a weak *in vivo* binding of this tracer to non-tangle tau lesions or even non-tau aggregates, in this study we have made a very careful selection of non-AD tauopathy cases with particularly robust non-PHF tau pathology, and of Lewy body and amyloid angiopathy cases that virtually lacked any tau pathology, other than incidental age-related tangles confined to the entorhinal cortex and limbic regions, to be able to draw the most accurate conclusions from our autoradiography and *in vitro* binding assays.

In conclusion, our results suggest that AV-1451 holds promise as a surrogate marker for the *in vivo* detection of tau pathology in the form of tangles and PHF-containing neurites in AD brains but also provide evidence of the relatively lower affinity of this tracer for tau lesions predominantly consisting of straight filaments in non-AD tauopathy cases, and of the existence of AV-1451 off-target binding to neuromelanin- and melanin-containing cells and to brain hemorraghic lesions. All together these data give important clues for the interpretation of the patterns of [F-18]-AV-1451 retention observed by *in vivo* neuroimaging. Future radiological-pathological studies on postmortem material from individuals scanned while alive should provide additional information for the reliable interpretation of change of the PHF-tau pathology burden in AD and its relationship to clinical progression of the disease, and the potential use of [F-18]-AV-1451 as an endpoint when testing therapies aimed at decreasing tangle burden or halting tau propagation across neural circuits in AD.

Acknowledgments

This study was supported by the ASISA Foundation (Madrid, Spain; M.M.); NIH National Institute of Neurological Disorders and Stroke (U01NS086659, M.D.N.); NIH National Institute of Mental Health (R01MH100350, M.D.N.); Harvard NeuroDiscovery Center (Boston, MA; C.R.V.); and NIH National Institute on Aging (AG005133, AG025204, W.E.K.; AG005133, AG025204, C.A.M.; AG025204, AG014449, M.D.I.; AG005134 and AG036694, T.G.-I.). We thank all the subjects who donated their brains to the MADRC; Avid Radiopharmaceuticals for providing AV-1451 fluorescent analogues and [H-3]-AV-1451; the Massachusetts General Hospital PET core for providing [F-18]-AV-1451; and Dr Peter Davies from the Feinstein Institute for Medical Research, North Shore LIJ for kindly sharing the PHF-1 antibody.

References

1. Xia CF, Arteaga J, Chen G, et al. [(18)F] T807, a novel tau positron emission tomography imaging agent for Alzheimer's disease. Alzheimer's & dementia: the journal of the Alzheimer's Association. 2013 Nov; 9(6):666–76.
2. Zhang W, Arteaga J, Cashion DK, et al. A highly selective and specific PET tracer for imaging of tau pathologies. Journal of Alzheimer's disease: JAD. 2012; 31(3):601–12. [PubMed: 22683529]
3. Chien DT, Bahri S, Szardenings AK, et al. Early clinical PET imaging results with the novel PHF-tau radioligand [F-18]-T807. Journal of Alzheimer's disease: JAD. 2013 Jan 1; 34(2):457–68. [PubMed: 23234879]
4. Cairns NJ, Bigio EH, Mackenzie IR, et al. Neuropathologic diagnostic and nosologic criteria for frontotemporal lobar degeneration: consensus of the Consortium for Frontotemporal Lobar Degeneration. Acta neuropathologica. 2007 Jul; 114(1):5–22. [PubMed: 17579875]
5. Hauw JJ, Daniel SE, Dickson D, et al. Preliminary NINDS neuropathologic criteria for Steele-Richardson-Olszewski syndrome (progressive supranuclear palsy). Neurology. 1994 Nov; 44(11): 2015–9. [PubMed: 7969952]
6. Armstrong MJ, Litvan I, Lang AE, et al. Criteria for the diagnosis of corticobasal degeneration. Neurology. 2013 Jan 29; 80(5):496–503. [PubMed: 23359374]
7. Tolnay M, Probst A. The neuropathological spectrum of neurodegenerative tauopathies. IUBMB life. 2003 Jun; 55(6):299–305. [PubMed: 12938731]
8. Murray ME, Kouri N, Lin WL, et al. Clinicopathologic assessment and imaging of tauopathies in neurodegenerative dementias. Alzheimer's research & therapy. 2014; 6(1):1.
9. Ferrer I, Lopez-Gonzalez I, Carmona M, et al. Glial and neuronal tau pathology in tauopathies: characterization of disease-specific phenotypes and tau pathology progression. Journal of neuropathology and experimental neurology. 2014 Jan; 73(1):81–97. [PubMed: 24335532]
10. Vonsattel JP, Del Amaya MP, Keller CE. Twenty-first century brain banking. Processing brains for research: the Columbia University methods. Acta neuropathologica. 2008 May; 115(5):509–32. [PubMed: 17985145]
11. Hyman BT, Phelps CH, Beach TG, et al. National Institute on Aging-Alzheimer's Association guidelines for the neuropathologic assessment of Alzheimer's disease. Alzheimer's & dementia: the journal of the Alzheimer's Association. 2012 Jan; 8(1):1–13.
12. Van Nostrand WE, Melchor JP, Cho HS, et al. Pathogenic effects of D23N Iowa mutant amyloid beta -protein. The Journal of biological chemistry. 2001 Aug 31; 276(35):32860–6. [PubMed: 11441013]
13. McKeith IG, Galasko D, Kosaka K, et al. Consensus guidelines for the clinical and pathologic diagnosis of dementia with Lewy bodies (DLB): report of the consortium on DLB international workshop. Neurology. 1996 Nov; 47(5):1113–24. [PubMed: 8909416]
14. Gilman S, Wenning GK, Low PA, et al. Second consensus statement on the diagnosis of multiple system atrophy. Neurology. 2008 Aug 26; 71(9):670–6. [PubMed: 18725592]
15. Hamilton R, Krauze M, Romkes M, et al. Pathologic and gene expression features of metastatic melanomas to the brain. Cancer. 2013 Aug 1; 119(15):2737–46. [PubMed: 23695963]
16. Koeppen AH, Michael SC, Li D, et al. The pathology of superficial siderosis of the central nervous system. Acta neuropathologica. 2008 Oct; 116(4):371–82. [PubMed: 18696091]

17. Santacruz K, Lewis J, Spires T, et al. Tau suppression in a neurodegenerative mouse model improves memory function. Science. 2005 Jul 15; 309(5733):476–81. [PubMed: 16020737]
18. Spires TL, Orne JD, SantaCruz K, et al. Region-specific dissociation of neuronal loss and neurofibrillary pathology in a mouse model of tauopathy. The American journal of pathology. 2006 May; 168(5):1598–607. [PubMed: 16651626]
19. Shoup TM, Yokell DL, Rice PA, et al. A concise radiosynthesis of the tau radiopharmaceutical, [(18) F] T807. Journal of labelled compounds & radiopharmaceuticals. 2013 Dec; 56(14):736–40. [PubMed: 24339014]
20. Gerfen CR. Basic neuroanatomical methods. Current protocols in neuroscience/editorial board. 2003 Aug. Jacqueline N Crawley [et al]. Chapter 1:Unit 1.
21. Caro LG, Van Tubergen RP, Kolb JA. High-resolution autoradiography. I. Methods. The Journal of cell biology. 1962 Nov.15:173–88. [PubMed: 14018772]
22. Woodbury DH, Beierwaltes WH. Fluorine-18 uptake and localization in soft tissue deposits of osteogenic sarcoma in rat and man. Journal of nuclear medicine: official publication, Society of Nuclear Medicine. 1967 Sep; 8(9):646–51.
23. Lewis DA, Campbell MJ, Terry RD, et al. Laminar and regional distributions of neurofibrillary tangles and neuritic plaques in Alzheimer's disease: a quantitative study of visual and auditory cortices. The Journal of neuroscience: the official journal of the Society for Neuroscience. 1987 Jun; 7(6):1799–808. [PubMed: 2439665]
24. Arnold SE, Hyman BT, Flory J, et al. The topographical and neuroanatomical distribution of neurofibrillary tangles and neuritic plaques in the cerebral cortex of patients with Alzheimer's disease. Cerebral cortex. 1991 Jan-Feb;1(1):103–16. [PubMed: 1822725]
25. Johnson, K.; Becker, A.; Sepulcre, J., et al. Tau PET: Initial experience with F18 T807; Presented at: 8th Human Amyloid Imaging; January 15–17, 2014; Miami, FL.
26. Sperling RA, Rentz DM, Johnson KA, et al. The A4 study: stopping AD before symptoms begin? Sci Transl Med. 2014; 6:228fs13.

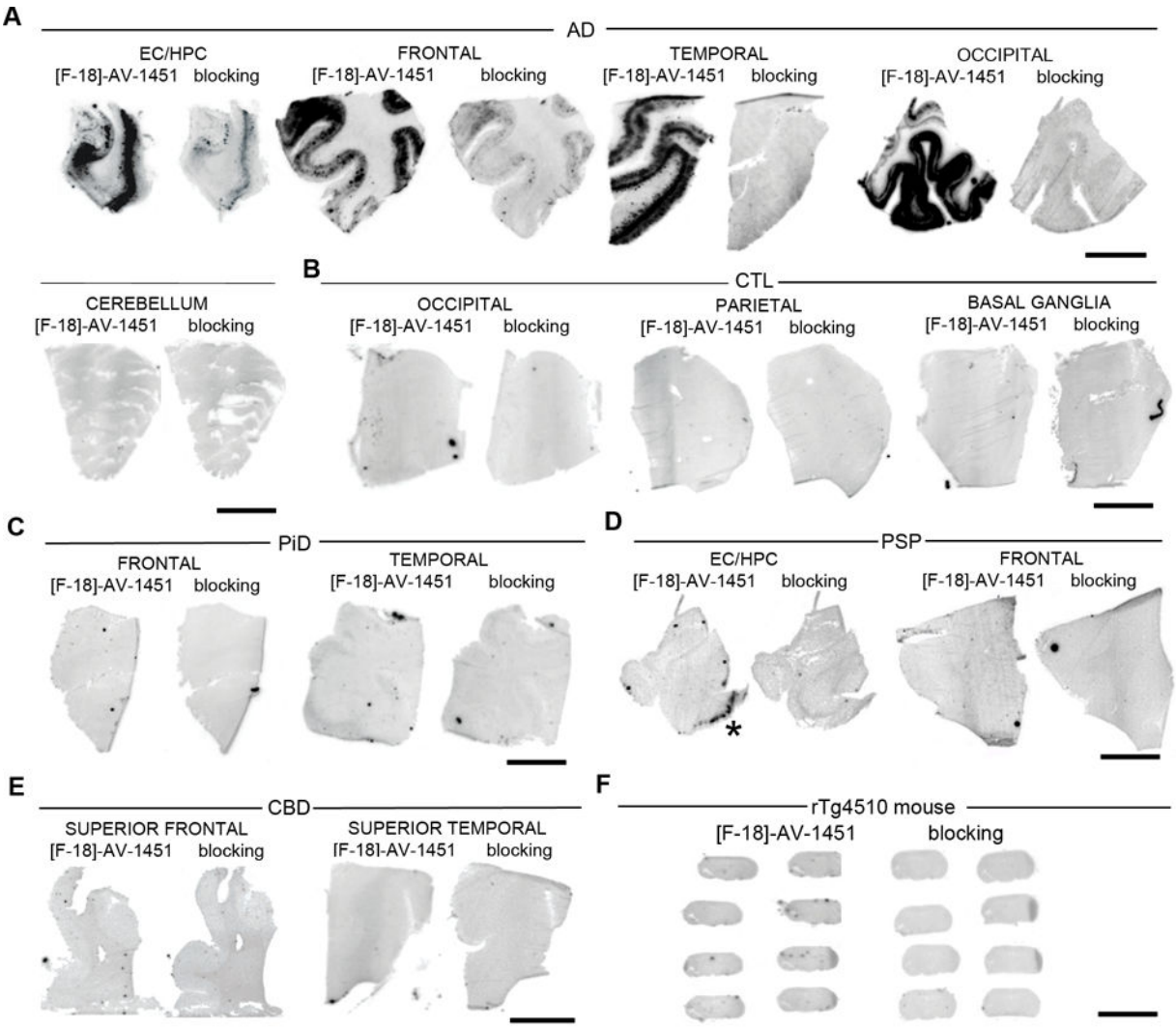

Figure 1.

[F-18]-AV-1451 phosphor screen images of brain slices from an AD case (A), a control (B), a PiD case (C), a PSP case (D), a CBD case (E) and a rTg4510 mouse brain (F). A strong [F-18]-AV-1451 binding was observed in cortical regions containing tangles and PHF-neurites from AD brains; the signal was blocked by adding unlabeled AV-1451 (A) and no [F-18]-AV-1451 signal was detected in the cerebellum (A). Slices from a control case free of pathology did not show detectable [F-18]-AV-1451 binding (B). [F-18]-AV-1451 binding was not detectable either in non-PHF tau-containing slices from a PiD case (C), a PSP case (D), a CBD case (E) and an rTg4510 mouse brain (F). Note that [F-18]-AV-1451 binding was confined to incidental age-related PHF-tangle pathology in superficial layers of EC in a PSP case (asterisk, D). Abbreviations: AD = Alzheimer's disease; CBD = corticobasal degeneration, CTL = control, EC = entorhinal cortex, HPC = hippocampus, NFT = neurofibrillary tangles; PiD = Pick's disease, PHF = paired helical filaments, PSP = progressive supranuclear palsy. Scale bar= 1 cm.

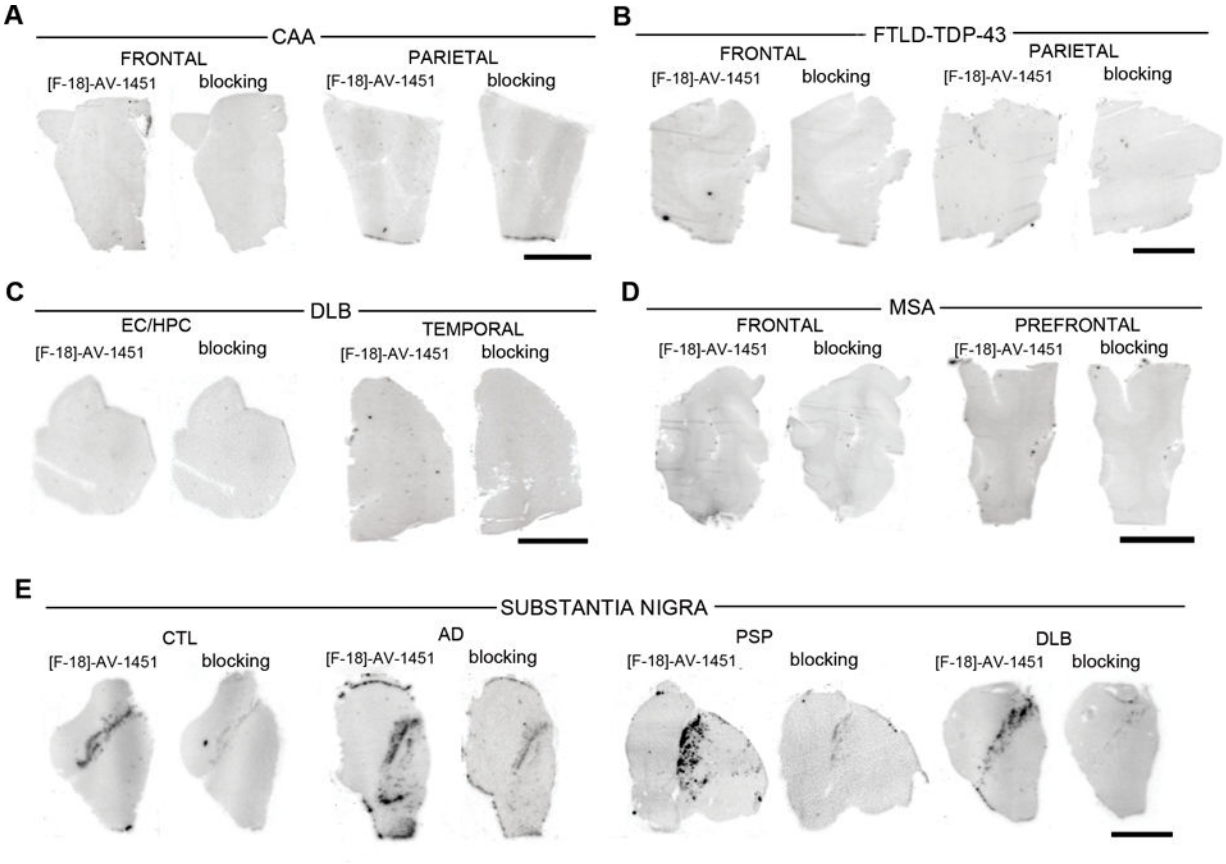

Figure 2.

[F-18]-AV-1451 phosphor screen images of brain slices from a CAA carrier of the D23N Iowa APP mutation (A), a FTLD-TDP-43 case (B), a DLB case (C), a MSA case (D) and midbrain containing slices from control, AD, PSP and DLB cases (E). No [F-18]-AV-1451 binding was detected in slices containing CAA lesions (A), TDP-43 inclusions (B), Lewy bodies (C) and glial α-synuclein inclusions (D). Strong [F-18]-AV-1451 signal was observed in the region corresponding to the substantia nigra in all cases studied regardless their pathological diagnosis. (E). Abbreviations: AD = Alzheimer's disease, APP = amyloid precursor protein, CAA = cerebral amyloid angiopathy, CTL = control, DLB = dementia with Lewy bodies, FTLD = frontotemporal lobar degeneration, MSA = multiple system atrophy, PSP = progressive supranuclear palsy, TDP-43 = TAR DNA binding protein 43. Scale bar= 1 cm.

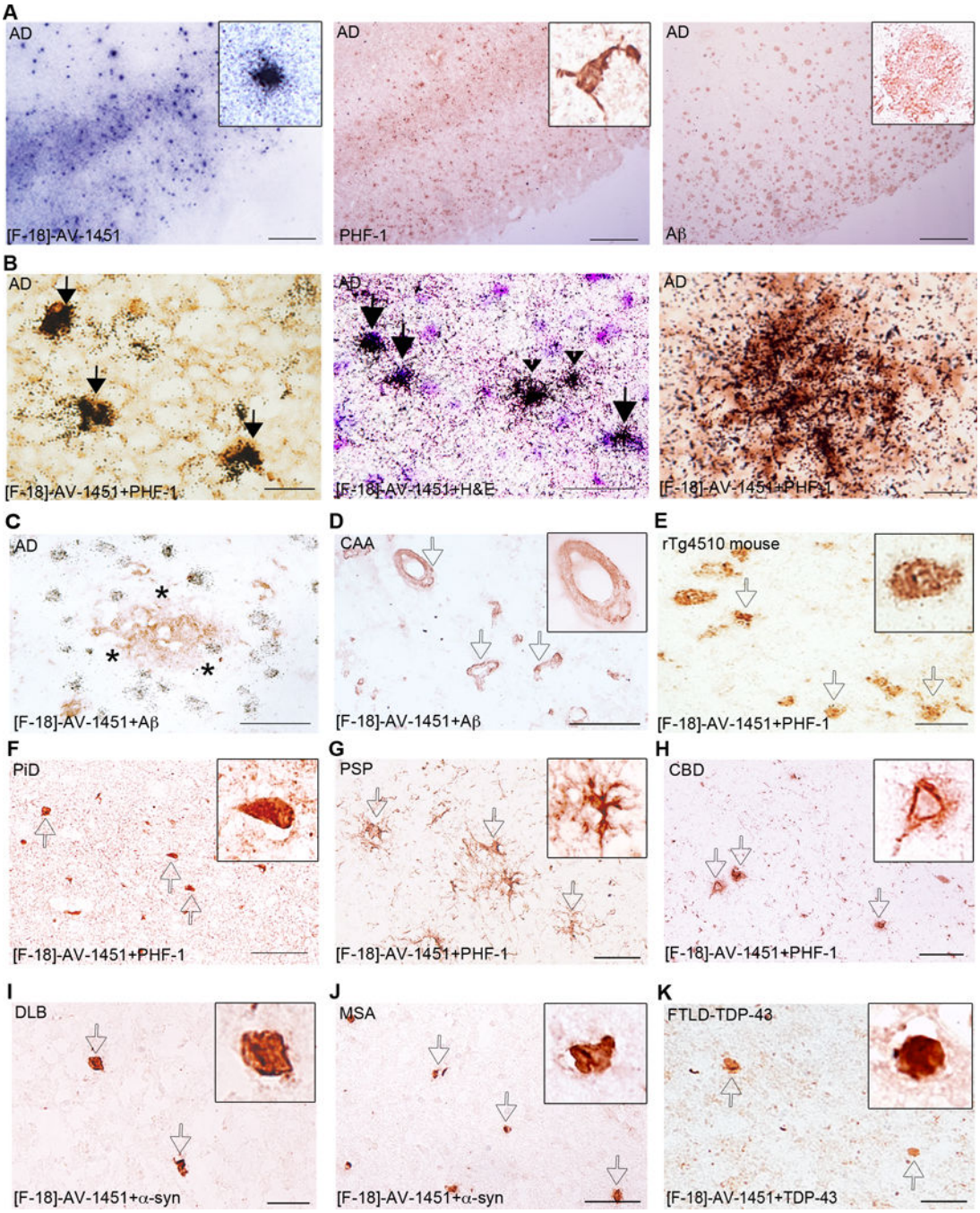

Figure 3.

[F-18]-AV-1451 nuclear emulsion autoradiography photomicrographs of brain slices from an AD case (A–C), a CAA carrier of the D23N Iowa APP mutation (D), a rTg4510 mouse (E), a PiD case (F), a PSP case (G) a CBD case (H), a DLB case (I), a MSA case (J) and a FTDL-TDP-43 case (K). Combined [F-18]-AV-1451 nuclear emulsion autoradiography followed by immunostaining with appropriate antibodies (B right and left panels, C–K) or H&E counter staining (B middle panel). The primary antibodies used were PHF-1 (kind gift of Dr. Peter Davies, A middle panel, B left and right panels, and E–H), anti-Aβ (A right

panel, C and D), anti α-synuclein (I and J) and anti-TDP-43 (K). [F-18]-AV-1451 nuclear emulsion autoradiography showed a strong cortical accumulation of silver grains in cortical layers III and V in AD brains (A, left panel) mirroring the pattern on adjacent slices of tau PHF-1 immunostaining (A, middle panel) but not the Aβ immunostaining (A, right panel). Accumulation of silver grains from the nuclear emulsion colocalized with PHF-1 stained tangles (solid arrows, B, left panel), both intraneuronal (solid arrows) and extraneuronal (black arrowheads, B middle panel) and PHF-tau containing neurites surrounding plaques in AD brains (empty arrows, B, right panel). No detectable accumulations of silver grains were observed in association with diffuse plaques in AD (asterisk, C), amyloid-containing vessels in CAA (empty arrows, D), tangles in Tg4510 mouse brains (empty arrows, E), Pick bodies in a PiD case (empty arrows, F), astrocytic plaques in a PSP case (empty arrows, G) or coiled bodies and globose tangles in a CBD case (empty arrows, H). No silver grains were detected in association with Lewy bodies in a DLB case (empty arrows, I), α-synuclein inclusions in a MSA case (empty arrows, J) or TDP-43 inclusions in a FTLD-TDP-43 case (empty arrows, K). Abbreviations: Aβ = amyloid-β, AD = Alzheimer's disease; APP = amyloid precursor protein, CAA = cerebral amyloid angiopathy, CBD = corticobasal degeneration, DLB = dementia with Lewy bodies, FTLD = frontotemporal lobar degeneration, H&E = hematoxylin and eosin, MSA = multiple system atrophy, PHF = paired helical filament, PiD = Pick's disease, PSP = progressive supranuclear palsy, TDP-43 = TAR DNA binding protein 43. Scale bar = 2 mm (A), 20 μm (B), 50 μm (C–K).

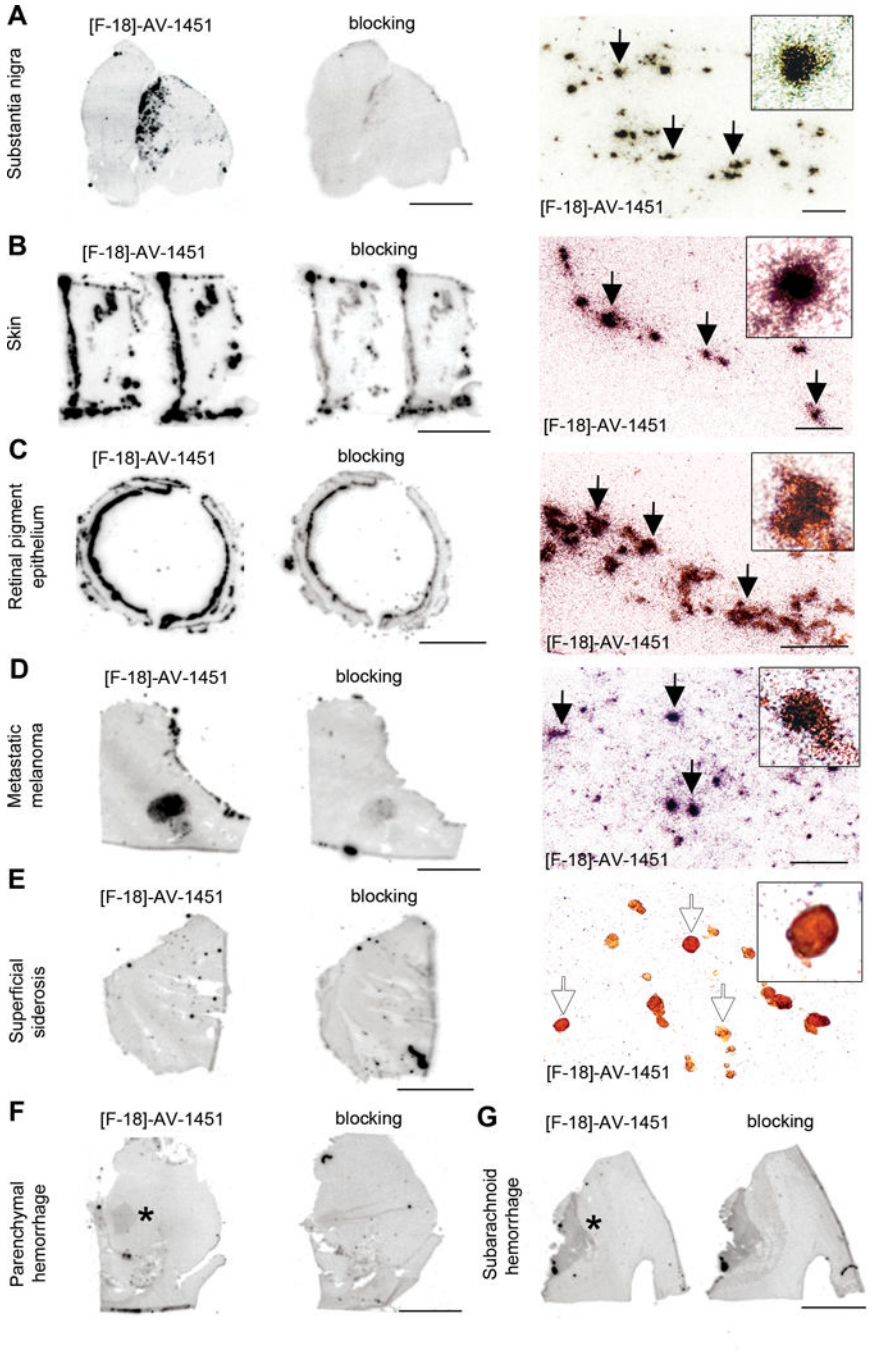

Figure 4.

[F-18]-AV-1451 phosphor screen and nuclear emulsion autoradiography images of slices containing substantia nigra in a PSP case (A), skin (B) and retinal pigment epithelium (C) in an AD case, metastatic melanoma (D), cerebellum in a superficial siderosis case (E), and parenchymal (F) and subarachnoid (G) hemorrhagic lesions. [F-18]-AV-1451 phosphor screen autoradiography images are displayed in A–E, left and middle panels, and F–G. [F-18]-AV-1451 nuclear emulsion autoradiography images are displayed in A–E, right panel. Strong [F-18]-AV-1451 binding was observed in neuromelanin-containing neurons of the

substantia nigra (A), skin melanocytes (B), neuromelanin containing granules in the retinal pigment epithelium (C) and malignant melanocytes from a metastatic melanoma (D). No detectable [F-18]-AV-1451 binding was observed in association with hemosiderin deposits in a superficial siderosis case (E). Mild [F-18]-AV-1451 binding was noticed in association with intraparenchymal (asterisk, F) and subarachnoid (asterisk, G) hemorrhagic lesions. Abbreviations: AD = Alzheimer's disease, PSP = progressive supranuclear palsy. Scale bar: 1cm (phosphor screen autoradiographic images), 50 μm (A, C, D right panels), 25 μm (B, E, right panels).

Table 1

Participants' characteristics

ID#	Clinical diagnosis	Pathological diagnosis	Age at death (years)	Gender	PMI (hours)	Braak & Braak (NFT)	CERAD score (neuritic plaques)	NIA-Reagan Institute criteria
#1	CTL	**Normal adult brain**	86	M	16	I	none	LP
#2	CTL	**Normal adult brain**	73	F	34	I	none	LP
#3	AD	**AD** + occipital **CAA**	64	F	38	VI	C	HP
#4	AD	**AD**	60	M	24	VI	C	HP
#5	AD	**AD**	56	F	N/A	VI	C	HP
#6	Memory, speech and gait difficulties, hand tremor	Diffuse **CAA** (D23N Iowa APP mutation)	45	M	N/A	I	none	LP
#7	FTD	**PiD**	62	M	24	I	A	LP
#8	FTD	**PiD**, type A	72	F	N/A	I	none	LP
#9	FTD	**PiD**, type A	82	M	N/A	II	A	LP
#10	PSP/FTD	**PSP**	63	F	12	II	none	LP
#11	PSP	**PSP**	69	M	45	II	none	LP
#12	PSP	**PSP**	68	M	80	II	none	LP
#13	CBD	**CBD**	80	M	N/A	I	none	LP
#14	FTD	**CBD**	83	M	N/A	I	A	LP
#15	DLB	**DLB**	76	M	17	II	none	LP
#16	DLB	**DLB** (Braak stage 5/6)	76	M	10	I	none	LP
#17	PDD	**DLB** (Braak stage 4/6)	83	M	9	III	none	LP
#18	MSA	**MSA**, cerebellar type (MSA-C)	60	F	32	II	none	LP
#19	MSA	**MSA**, Parkinsonian type (MSA-P)	80	M	25	I	none	LP
#20	FTD	**FTLD-TDP-43**, type A	69	F	N/A	I	none	LP
#21	AD	**Metastatic melanoma** in frontal and parietal lobes bilaterally	75	M	35	V	B	IP
#22	Dementia, ataxia, dysphagia, hearing loss	**Superficial siderosis**	68	M	12	I	A	LP
#23	Headache	**Subarachnoid hemorrhage**	92	F	N/A	IV	A	IP
#24	N/A	**Parenchymal hemorrhage**	75	M	N/A	I	none	LP

Abbreviations: AD = Alzheimer's disease, APP = amyloid precursor protein, CAA = cerebral amyloid angiopathy, CBD = corticobasal degeneration, CERAD = Consortium to establish a Registry for Alzheimer's disease, CTL = control subject, DLB = dementia with Lewy bodies, F = female, FTLD = frontotemporal lobar degeneration, HP = high probability, IP =intermediate probability, LP = low probability, M = male, MSA= multiple systemic atrophy, NFT = neurofibrillary tangles, NIA = National Institute of Aging, N/A = non available, PiD = Pick disease, PMI = postmortem interval, PSP = progressive supranuclear palsy, TDP-43 = TAR DNA binding protein 43

Table 2

[H-3]-AV-1451 *in vitro* binding assays

Pathologic diagnosis	n	Brain region	[H-3]- AV-1451 (pmol/gr)	Pathologic diagnosis	n	Brain region	[H-3]- AV-1451 (pmol/gr)
CTL	2	Parietal cortex	132	PSP	2	Substantia nigra	92
		Temporal cortex	180			Thalamus	240
		Occipital cortex	144			Pons	111
		HPC/EC	165			Basal ganglia	205
		Substantia nigra	226	CBD	2	Frontal cortex	106–210
		Cerebellum	238			Temporal cortex	137–177
		Basal ganglia	179	DLB	2	Parietal cortex	152
AD	3	Frontal cortex	198			Occipital cortex	238
		Parietal cortex	258			Substantia nigra	139–238
		Occipital cortex	301			Cerebellum	183
		HPC/EC	299			Basal ganglia	141
		Substantia nigra	88–220	MSA	1	Frontal cortex	168–210
		Cerebellum	219	FTLD-TDP-43	2	Frontal cortex	125
		Basal ganglia	124			Parietal cortex	208
CAA	1	Frontal cortex	142	Metastatic melanoma	1	Frontal lobe	611
		Parietal cortex	248			Parietal lobe	451
		Occipital cortex	259	Superficial siderosis	1	Cerebellum	270
PiD	3	Frontal cortex	94–207	Subarachnoid hemorrhage	1	Temporal cortex	652
		Temporal cortex	148			Parietal cortex	434
		HPC/EC	300	rTg4510 mice	2	Whole brain	167–180
		Substantia nigra	234	WT mice	2	Whole brain	145–183
		Cerebellum	244				
		Basal ganglia	162				

Ann Neurol. Author manuscript; available in PMC 2016 November 01.

Abbreviations: AD = Alzheimer's disease, CAA = cerebral amyloid angiopathy, CBD = corticobasal degeneration, CTL = control subject, DLB = dementia with Lewy bodies, FTLD = frontotemporal lobar degeneration; HPC/EC = hippocampus/entorhinal cortex, MSA= multiple systemic atrophy, N/A = non available, PiD = Pick disease, PSP = progressive supranuclear palsy, TDP-43 = TAR DNA binding protein 43, WT = wild type.